Multi-Access Interference Processes Are Self-Similar in Multimedia CDMA Cellular Networks*

Junshan Zhang
Dept. of EE
Arizona State University
Tempe, AZ 85287, USA
email: junshan.zhang@asu.edu

Takis Konstantopoulos
Dept. of ECE
University of Texas at Austin
Austin, TX 78712, USA
email: takis@ece.utexas.edu

Abstract

We consider bursty data communications in code-division-multiple-access (CDMA) cellular networks. The significant fluctuation of the co-channel multi-access interference (MAI) in such systems makes it very challenging to carry out radio resource management. A main goal of this paper is to obtain a fundamental understanding of the temporal correlation structure of the MAI, which plays a crucial role in effective resource allocation. To this end, we take a cross-layer design approach, and characterize the stochastic MAI process while taking into account both the burstiness of data traffic and time varying channel conditions. Our main results reveal that under standard assumptions on ON/OFF traffic flows and fading channels, the MAI process exhibits scale-invariant burstiness and is "self-similar" (with Hurst parameter $1/2 < H < 1$), in both the uplink and the downlink cases. The MAI self-similarity indicates that the MAI levels are long-range dependent and therefore there exists a nontrivial predictive MAI structure across multiple time scales. The predictive MAI structure can be utilized for effective interference management through dynamic resource allocation. We illustrate this via a rate control scheme based on the MAI prediction, and our results show that the performance gain is substantial. The exploitation of the MAI temporal correlation structure for resource allocation parallels and complements multiuser detection which utilizes the MAI snapshot structure at the symbol level.

Keywords: CDMA, multi-access interference, heavy-tailed, self-similarity, long-range dependence, resource allocation, cross-layer design.

*This research is supported in part by the National Science foundation through grants ANI-0208135, ANI-0238550 & ANI-9903495, and by a grant from the Intel Research Council.

1 Introduction

The coming generation of tetherless communication technologies promises a giant leap forward in information accessibility. Fueled by the great demand for wireless Internet access, it is expected that third generation (3G) systems and beyond will be able to provide a wide variety of services ranging from low-data-rate services, such as paging and email, to very high-data-rate multimedia services such as e-commerce, web browsing, and video streaming. Indeed, the 3G standards require the support of high-speed multimedia traffic in both the reverse and forward channels [1]. Accommodation of flexible data applications with such a wide range in wireless networks is challenging. There is a rapidly growing consensus that developing network-level solutions that take advantage of the interplay between the communication channel and the upper protocol layers would yield significant performance gains. It is then of vital importance to investigate new methods of modeling, analysis, and simulation that incorporate an understanding both of network and channel characteristics.

In this paper, we study the transmission of bursty data traffic in wideband code-division-multiple-access (CDMA) networks. Since CDMA systems are interference-limited, a key to effective resource management is to obtain accurate MAI prediction. A major challenge in such systems is the significant fluctuation of the co-channel multi-access interference (MAI), induced by both traffic burstiness and channel variation. It is of great interest to ask the following questions. Does there exist a predictive MAI structure, and if yes, how do we make use of it for interference prediction? How can we exploit interference prediction to improve resource management? Although there has been tremendous research on characterizing the marginal distribution of the MAI [11, 16, 25, 37, 52, 57, 59], the MAI temporal correlation structure has been barely explored and is not well understood. Indeed, the MAI, particularly the intercell MAI, is known to be very difficult to cope with.

A main goal of this paper is to provide some first steps in understanding the predictive MAI temporal structure so as to establish a framework for utilizing MAI prediction for resource management. Specifically, we first model the MAI from a stochastic process perspective (in contrast to studying marginal distributions). This model integrates explicitly both the characteristics of fading channels and the burstiness of data traffic, and has a flavor of so-called "cross-layer design". Then we characterize the MAI process, via a marriage of tools from the network traffic engineering and communication theory. Throughout we assume that users experience (stationary) fading. Under standard assumptions on the ON/OFF-periods of the multimedia traffic (see, e.g., [55]) and on the correlation functions of fading channels, our findings reveal that the MAI processes, in both the uplink and the downlink, exhibit scale-invariant burstiness and are asymptotically "self-similar".

We now briefly discuss the asymptotic self-similarity of the MAI process. We note that the time-varying channel conditions make the characterization of the MAI processes highly nontrivial. In particular, for the uplink MAI process, time-varying fading dictates time-varying rewards in the ON-periods, and a second-order analysis generalizing [46] is required to show that the uplink MAI can be well modelled as a fractional Brownian motion. In contrast, for the downlink case, we cannot hope that the downlink MAI can be approximated by a fractional Brownian motion or even a Gaussian process (cf. [46]), because the fading factor in the MAI process is common for all users in one cell

and there might be strong correlation between the summands of the MAI. The issue of scaling is nontrivial in the non-Gaussian world in general (see, e.g.,[21, 30]). To this end, we need to invoke the tool on Skorohod's Representation, namely "the method of a single probability space" [43], to characterize the downlink MAI process. We will elaborate further on this in Section 4.

Our approach takes into account simultaneously the burstiness of data traffic, fading and the changes of other network parameters, and opens a new dimension to the understanding of the MAI temporal structure. In particular, the MAI self-similarity, with Hurst parameter $1/2 < H < 1$, indicates directly that the MAI is long-range dependent. Therefore, the MAI is strongly correlated at coarser time scales, that is, there exists a nontrivial MAI temporal correlation structure. The predictive MAI temporal structure can then be utilized for effective interference management through dynamic resource allocation, such as rate adaptation, admission control, and energy-efficient transmission. To illustrate the utility of the MAI self-similarity, we provide a simple example in which the MAI temporal correlation structure is exploited for interference prediction and then for rate adaptation to ameliorate the system performance. Our numerical examples illustrate that the throughput gain of rate adaptation by using the MAI temporal structure is significant.

The above exploitation of the predictive MAI temporal structure is reminiscent of multiuser detection [51], which exploits the MAI snapshot structure at the *symbol level*, a much finer time scale, whereas rate control and admission control decisions are taken on *coarser time scales*. These two exploitations of the MAI structure complement each other. We emphasize that our findings show that particularly the intercell MAI is long-range dependent, and that the MAI temporal structure is especially useful for managing the intercell MAI (which is known to be difficult).

As pointed out above, in related work there has been a great deal of research on the marginal distribution of MAI. In particular, the so-called standard Gaussian approximation (SGA) for MAI in systems with matched filter receivers dates back to very early works [37, 57]. The improved Gaussian approximation (IGA) for random signature sequences has been reported in [25, 32, 16]. Generalization to multipath fading, imperfect power control, and non-coherent demodulation can be found in [11, 19, 24, 38, 50, 52] and the references therein. An Alpha-stable interference model has been developed for a collection of Poisson-distributed bursty transmitters in [18]. Similar models have been proposed and rigorously justified for communication networks [22, 30]. In contrast to the MF receiver, the MMSE receiver exploits the MAI structure provided by the signature sequences and received powers of the interferers. Since short signature sequences are more relevant for implementing the MMSE receiver [15, 17, 28], the more interesting quantity in this case is the conditional distribution of the output MAI for a given set of signatures. A general study can be found in [36, 58, 59], which have established the normality of output MAI in a large network with MMSE receivers. Extension of the results in [59] can be found in recent work [14].

We note that the issue of macroscopic model choices, which is the subject of this paper, is often a nontrivial matter, because different scalings may lead to different results (see, e.g., [21, 23, 30, 47] for a treatment of this issue on models that arise in connection to network traffic). In particular, the choice of the macroscopic model depends on what is being approximated—the process itself or a functional of it. In this paper, we believe that it is the MAI process itself that is of primary

importance in CDMA cellular networks, and therefore approximate it macroscopically by using self-similar models. During the final stage of the preparation of this paper, we were informed of the interesting results in [56] that provide conditions under which the interfering signal in a Poisson Field of Interferers becomes m-dependent, ϕ-mixing or long-range dependent. One key difference between [56] and this paper lies in the fact that [56] considers the interfering signals in a Poisson field, and the results therein would be useful for the optimum receiver design at small time scales. In contrast, we focus on the temporal correlation structure of the MAI power (the power of the interfering signal) in CDMA networks with ON/OFF traffic flows, and the corresponding structures can then be utilized for effective interference management through dynamic resource allocation at coarser time scales.

The organization of the remainder of this paper is as follows. The next section contains our model description for the MAI processes in both the uplink and the downlink transmissions. In Section 3 we provide some necessary background. We present our main results on the MAI self-similarity in Section 4. We provide in Section 5 some discussions on the utility of MAI self-similarity in adaptive resource allocation in CDMA systems. In Section 6, we provide numerical examples to illustrate our findings. The conclusions can be found in Section 7.

2 Modeling MAI: A Stochastic Process View

Consider a cellular CDMA network with many ON/OFF data users in each cell (cf. [31]). In view of the bursty nature of multimedia traffic, we follow [55] and assume that the ON- or OFF-periods are *heavy-tailed* and exhibit the *Noah Effect*, i.e., have high variability or infinite variance (see [55] and the references therein). Intuitively, the Noah Effect for an individual ON/OFF source model yields ON- and OFF-periods that can be very large with non-negligible probability.

Let J be the number of cells under consideration. Let $\mathcal{U}$ be the set of users in such a network. Roughly speaking, cells can be treated as disjoint sets of users. So $\mathcal{U}$ is partitioned into cells $C_1, \ldots, C_J$. Let K_j be the number of users in C_j, for $j = 1, \ldots, J$. The transmission framework is direct-sequence CDMA, indicating that the interference to any user's transmission at any time is the superposition of the effects of all other current active transmissions in the network. In order to understand the temporal correlation structure of the interference, we investigate the MAI from a stochastic process perspective.

2.1 The MAI Process in the Uplink

We start with modeling the MAI process in the uplink. We assume frequency-flat fading (see Section 4.3 for extensions to frequency-selective fading channels). Without loss of generality, consider a typical user 1 in cell C_1. Assume that the matched filter is employed to demodulate the received signal. First consider the interference process to user 1 generated by user k in cell C_i (see Figure 1). By assumption, user k in cell C_i is an ON/OFF user, i.e., it is active over ON intervals, which are interlaced with OFF intervals. Let $X_{k,i}(t)$ be its activity indicator at time t, whereby $X_{k,i}(t) = 1$ if

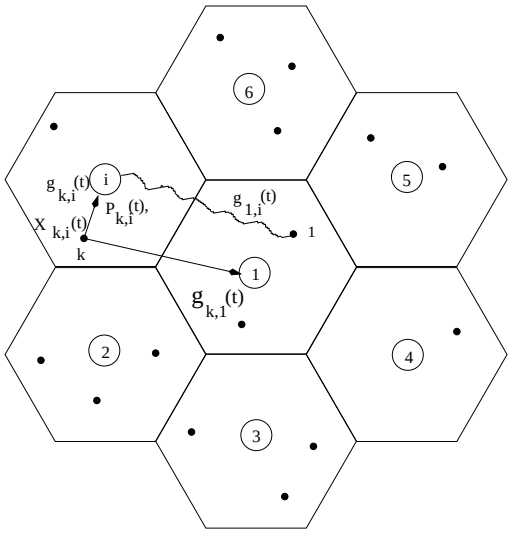

Figure 1: *A simplified cellular system model: Users are denoted by black dots and cell sites by circles. The interference to user 1, produced by user k in cell i, is the product of three terms, the activity indicator of user k, the transmission power of user k, and a term involving the fading process (uplink: the fading effect from this user to user* 1*; downlink: the fading effect from the cell site i to user* 1*.)*

and only if the user is ON at time t, and, otherwise, it is zero. Also, let $P_{k,i}(t)$ be the transmission power of user k in cell i at time t, and $g_{k,i}(t)$ denote the channel gain (or fading effects) from user k in cell i to cell site i.

We briefly review the fading channels and transmission powers. Roughly speaking, fading effects can be categorized into large time-scale (slow) fading and small time-scale (fast) fading, which are due to different mechanisms in the wireless media. Large-scale fading, including distance-related attenuation and shadowing effects, causes slow variation of signal strength, whereas small-scale fading causes rapid variation of signal strength. For mathematical tractability, we impose that the fading is independent and identically distributed across the users in the same cell [51].

Throughout this paper, we assume that the power allocation of each user is carried out based on the slow fading. Recall that the MAI to any user's transmission at any time is the superposition of the "contributed signals" of all other current active transmissions in the network. Then, the intracell MAI at time t (at the receiver for user 1 in cell 1—the user under consideration) is given by

$$\mathcal{I}_{1,1} = \sum_{k\in C_1, k\neq 1} P_{k,1}(t)h_{k,1}(t)g'_{k,1}(t)X_{k,1}(t) \ = \sum_{k\in C_1, k\neq 1} g'_{k,1}(t)\bar{P}X_{k,1}(t) \tag{1}$$

where $h_{k,1}$ denotes the slow fading and $g'_{k,1}(t)$ is the fast fading, and $\bar{P}$ is the target received power. Moreover, the intercell MAI at time t due to the users in cell i ($i \neq 1$), denoted $\mathcal{I}_{1,i}$, is given by

$$\mathcal{I}_{1,i}(t) = \sum_{k\in C_i} P_{k,i}(t)g_{k,1}(t)X_{k,i}(t) \tag{2}$$

where $g_{k,1}(t)$ stands for the overall channel gain from user k in cell i to cell cite 1, which is independent from $g_{k,i}(t)$ (see Figure 1). Accordingly, it is reasonable to assume that $g_{k,1}(t)$ and

$P_{k,i}(t)$ are independent, because $P_{k,i}(t)$ depends on $g_{k,i}(t)$ only. In summary, the total MAI is given by $\sum_{i=1}^{J}\sum_{k\in C_1} P_{k,1}(t)g_{k,1}(t)X_{k,1}(t)$, where it is understood that for the intracell MAI, $P_{k,1}(t)g_{k,1}(t) = g'_{k,1}(t)\bar{P}$.

In a network with many users, the signal-to-interference-plus-noise (SINR) is given by

$$\mathrm{SINR}_{1,1}(t) = \frac{P_{1,1}(t)g_{1,1}(t)}{\sigma^2 + \frac{R_{1,1}(t)}{W}\sum_{i=1}^{J}\mathcal{I}_{1,i}(t)}, \tag{3}$$

where $R_{1,1}(t)$ is the transmission rate of user 1 in cell 1, W denotes the bandwidth, and σ^2 is the variance of the ambient additive white Gaussian noise. The total MAI, $\sum_{i=1}^{J}\mathcal{I}_{1,i}(t)$, consisting of both intercell interference and intracell interference, is a key parameter that limits the capacity of CDMA systems. It is worth noting that the *intercell* MAI always exists, even though in theory the *intracell* MAI $\mathcal{I}_{1,1}$ can be eliminated by using orthogonal spreading in downlink if multipath does not exist [12, 39].

2.2 The MAI Process in the Downlink

Next, we turn to model the MAI Process in the downlink. A key feature differentiating downlink transmissions from uplink transmissions is that the signals of all users in the same cell are aggregated and transmitted using the same antenna so the channel gain (to the user under consideration) is exactly the same. Let $g_{1,i}(t)$ denote the channel gain from the base station in cell i to the user under consideration. Let $P_{k,i}(t)$ be the transmission power (in the downlink) of user k in cell i at time t. *We note that the system parameters in the downlink, including $g_{1,i}(t)$ and $P_{k,i}(t)$, are not the same as the corresponding ones in the uplink (indeed they are independent). We "abuse" the notation for the sake of simplicity.* Again, we assume that the power allocation is carried out based on the slow fading. Then the intracell MAI is given by

$$\mathcal{I}_{1,1} = \left(\sum_{k\in C_1, k\neq 1} P_{k,1}(t)X_{k,1}(t)\right) g_{1,1}(t) \tag{4}$$

and the intercell MAI due to the transmissions in cell i ($i \neq 1$), denoted $\boldsymbol{I}_{1,i}$, is given by

$$\boldsymbol{I}_{1,i}(t) = \left(\sum_{k\in C_i} P_{k,i}(t)X_{k,i}(t)\right) g_{1,i}(t) \tag{5}$$

The SINR can then be approximated as

$$\mathrm{SINR}_{1,1}(t) = \frac{P_{1,1}(t)g_{1,1}(t)}{\sigma^2 + \frac{R_{1,1}(t)}{W}\sum_{i=1}^{J}\boldsymbol{I}_{1,i}(t)}.$$

3 Background

Multimedia traffic in emerging communications applications, such as web browsing and video streaming, is highly bursty, i.e., the required transmission time has a wide range and can be very large with

non-negligible probability. A quantitative metric of data burstiness is *heavy-tailedness*. It has been shown that a variety of traffic, including TCP connections, streaming video, and web traffic are well modeled as heavy tailed (see, e.g., [8, 10]). In what follows, we give the definitions of the heavy tailed distribution and self-similar process [2, 3, 8].

3.1 Heavy-Tailed Distribution and Self-Similar Process

Definition 3.1 A random variable X has a *heavy-tailed* distribution if

$$\Pr\{X > x\} \sim \ell x^{-\alpha}$$

as $x \to \infty$, where $0 < \alpha < 2$ and ℓ is a constant. (The notation $f(x) \sim g(x)$, as $x \to \infty$, means that $\lim_{x\to\infty} f(x)/g(x) = 1$.)

Roughly speaking, the asymptotic shape of the tail of the distribution obeys a power law.

More generally, we could say that X is heavy-tailed if, for some $1 < \alpha < 2$, $\Pr\{X > x\} \sim x^{-\alpha}L(x)$, as $x \to \infty$, where $L(x)$ is a slowly-varying function at ∞, *viz.,* $\lim_{x\to\infty} L(\lambda x)/L(x) = 1$, for all $\lambda > 0$. However, for the purposes of this paper, we take $L(x) = 1$.

Definition 3.2 A random process $Y = \{Y(t), t \geq 0\}$ is *self-similar* (with Hurst parameter H, $0 < H < 1$) if it satisfies the condition:

$$\{Y(t), t \geq 0\} \stackrel{d}{=} \{a^{-H}Y(at), t \geq 0\}, \quad \forall a > 0,$$

where the equality is in the sense of (at least finite-dimensional) distributions.

There are many self-similar processes, the most common ones being the fractional Brownian motion and linear fractional stable motion [42]. We note that fractional Brownian motion is the only self-similar Gaussian process with $0 < H < 1$.

In the following, we also give the definition of a "weaker" but widely used notion of self-similarity, namely second-order self-similarity (see [21] and the references therein).

Definition 3.3 A stochastic process $\{Y(t), t \geq 0\}$, with finite variance for all t, is asymptotically second-order self-similar if and only if there exists a positive function a_T, $T > 0$, such that the covariance function of

$$\left\{ \frac{1}{a_T} Y(Tt),\ t \geq 0 \right\}$$

has a limit as $T \to \infty$, and the limit is also a covariance function.

It follows that if such an a_T exists then a_T must be a regularly varying function of index H. The same index is said to be the index of the second-order self-similarity of the process $\{Y(t), t \geq 0\}$.

It has been shown that the network traffic can be effectively characterized by self-similar models, that is, the network traffic exhibits scale-invariant burstiness over a wide range of time scales (see [7, 26, 34, 46, 54, 55] and the references therein). In this paper, we show that the *accumulated MAI* is self-similar. Specifically, The MAI, consisting of a superposition of the interference processes from both the intercell and intracell interference, is shown to be asymptotically self-similar.

3.2 Probability Laws of User ON/OFF-Periods

To specify the distributions of the ON/OFF-periods, we let

$$f_1(x), \quad F_1(x) = \int_0^x f_1(u)du, \quad F_{1c}(x) = 1 - F_1(x),$$

$$\mu_1 = \int_0^\infty x f_1(x)dx, \quad \sigma_1^2 = \int_0^\infty (x-\mu_1)^2 f_1(x)dx$$

denote the probability density function, cumulative distribution function, complementary (or tail) distribution, mean length and variance (if it exists) of an ON-period, and let f_2, F_2, F_{2c}, μ_2, σ_2^2 correspond to an OFF-period. Following [55], we assume that as $x \to \infty$,

(A1) either $F_{1c}(x) \sim \ell_1 x^{-\alpha_1}$ with $1 < \alpha_1 < 2$ or $\sigma_1^2 < \infty$,

(A2) either $F_{2c}(x) \sim \ell_2 x^{-\alpha_2}$ with $1 < \alpha_2 < 2$ or $\sigma_2^2 < \infty$,

where ℓ_j is a constant, $j = 1, 2$. Following [46], we set $\alpha_j = 2$ when $\sigma_j^2 < \infty$. Define

$$\alpha_{\min} \stackrel{\triangle}{=} \min(\alpha_1, \alpha_2),$$

$$H \stackrel{\triangle}{=} \frac{3 - \alpha_{\min}}{2}.$$

Again, we note that since our main goal is to diagnose the MAI self-similarity and identify the corresponding Hurst parameter, our ON/OFF model does not include the slowly varying functions in [55]. The extension to the latter case is easy, as will be evident in the proof of our main result.

For simplicity, we impose the following assumption:

Condition 1 The distributions of ON/OFF-periods are the same for all users.

Our results can be easily generalized to the cases where the distributions of ON/OFF-periods are different across users by using [46, Theorem 2].

4 Main Results on MAI Self-Similarity

In the following, we show that the MAI process is asymptotically self-similar. As in [31], we let the bandwidth W be large (tend to infinity), and assume that K_i grows linearly with W, that is, the ratio $\beta_i = K_i/W$ remains fixed, for $i = 1, \ldots, J$. Let T denote the time scale (time window). We show that as both T and W increase, the MAI, consisting of both the intercell and intracell interference, is self-similar. It is clear from (2) and (5) that the interference process from a user, say user k in cell j, is a product of its ON/OFF process $X_{k,j}(t)$ and its corresponding fading process ($g_{k,j}(t)$ in the uplink and $g_{1,j}(t)$ in the downlink). The fading coefficients can then be treated as "rewards" for the underlying renewal process (i.e., the ON/OFF process). It has been shown that the superposition of many ON/OFF heavy-tailed Ethernet sources is self-similar [7, 23, 27, 54], where the "rewards" in each ON-period are constant. Clearly, time-varying fading dictates time-varying rewards in the ON-periods, making the understanding of the MAI process more challenging and

nontrivial. In particular, our characterization of the downlink MAI process involves "the method of a single probability space" [43].

Our approach can also be applied to model the aggregated network traffic made up by many individual sources or source-destination pairs, where each individual source is allowed to generate time-varying traffic (e.g., variable bit rate sources). In this sense, our results can also be viewed as a generalization of results in [23, 46, 55], although the models under consideration are different.

Now, we elaborate further on what we mean by asymptotic self-similarity. Let $p(t)$ be a random process, representing interference, such as the MAI process in this paper. It is clear that $p(t)$ depends on the total bandwidth W. As W increases, $p(t)$ "grows" because more users can be accommodated. If there exist indices $0 < H < 1$, $\ell > 0$, such that $T^{-H}W^{-\ell}\int_0^{Tt} p(s)ds$ converges in distribution as W and T go to infinity (in that order) to a self-similar process, we say that $p(t)$ is asymptotically self-similar. Letting $Z(t)$ denote this limiting self-similar process we can then roughly write that $\int_0^{Tt} p(s)ds \stackrel{d}{=} W^{\ell}T^{H}Z(t) \stackrel{d}{=} W^{\ell}Z(Tt)$. In other words, $\int_0^{t} p(s)ds \stackrel{d}{=} W^{\ell}Z(t)$, where the equality in distribution is approximate and hold for large W and large t. Thus, $p(t)$ can be *macroscopically* modeled by the formal derivative of a self-similar process.

4.1 MAI Self-Similarity in the Uplink

We first characterize the MAI process in the uplink. To this end, we impose the following assumption on the correlation function of the fading and the transmission power:

Condition 2 The correlation functions of $g_{k,i}(t)$ and $P_{k,i}(t)$, denoted as $\varrho_{k,i}(u)$ and $\vartheta_{k,i}(u)$, are $o(u^{2H-2})$ as $u \to \infty$, for $k \in C_i$ and $i = 1, \ldots, J$.

We note that Condition 2 holds in many fading channel models of practical interest because typically the coherence time of fast fading is on the order of mini-seconds and that of slow fading is on the order of hundreds of mini-seconds. For example, in a block fading channel, channel gains are assumed to be constant for some symbol period (say T_b), after which they change to new independent random values and maintain constant for another period T_b, and so on [4, 29]. It follows that the corresponding correlation function $\varrho(u) = 0$ for $u > T_b$, which simply indicates that $\varrho(u)$ satisfies Condition 2. Another example is log-normal shadowing, which has been shown, based on measurements (in dB), to be effectively characterized by an autoregressive (AR) model [13, 44]:

$$g((n+1)T_f) = \xi g(nT_f) + (1-\xi)\nu_n \tag{6}$$

where $\xi \in (0,1)$ and ν_n is zero-mean white Gaussian noise, and T_f is some time constant. It can be shown that the correlation function $\varrho(u)$, given in [13], satisfies Condition 2. Recall that the power allocation is done based on the slow fading. In light of the coherence time of slow fading and the duration of ON/OFF-periods, the regularity condition on the transmission power is applicable to many practical wireless systems.

We are now ready to present our main result on the MAI process in the uplink.

Theorem 4.1 (MAI Self-Similarity in Uplink) *Suppose that Conditions 1 and 2 hold. Then, as both W and T increase,*

a) The normalized accumulated MAI from cell i, $\{T^{-H}W^{-1/2}\int_0^{Tt}(\mathcal{I}_{1,i}(u)-\mathbb{E}[\mathcal{I}_{1,i}(u)])du,\ t\geq 0\}$, converges in the sense of finite-dimensional distributions to a fractional Brownian motion with Hurst parameter $H=(3-\alpha_{\min})/2$.

b) The normalized total accumulated MAI, $\{T^{-H}W^{-1/2}\int_0^{Tt}(\sum_{i=1}^{J}\mathcal{I}_{1,i}(u) - \mathbb{E}[\sum_{i=1}^{J}\mathcal{I}_{1,i}(u)])\ du,\ t\geq 0\}$, converges in the sense of finite-dimensional distributions to a fractional Brownian motion with Hurst parameter $H=(3-\alpha_{\min})/2$.

Remarks: A Fractional Brownian motion $B_H(t)$ is a Gaussian process with mean zero, stationary increments, and covariance function

$$\mathbb{E}[B_H(t)B_H(s)]=\frac{1}{2}\left\{s^{2H}+t^{2H}-|t-s|^{2H}\right\}.$$

The corresponding increments of fractional Brownian motion, $G_j=B_H(j)-B_H(j-1)$, for $j=1,2,\cdots$, are called fractional Gaussian noise and are strongly correlated [3, 46]:

$$\mathbb{E}[G(j)G(j+k)]\sim \ell_1 k^{2H-2}\ \text{ as }\ k\to\infty. \tag{7}$$

Based on the (7), we have the following interpretation of Theorem 4.1. The asymptotic self-similarity of the MAI process in the uplink implies that the MAI exhibits long-range dependence at coarse time scales, i.e., there are extended periods of either strong or weak interference. Without suitable adaptive resource allocation, the MAI self-similarity (with Hurst parameter $1/2<H<1$) indicates extended periods of poor SINR when the MAI is strong, or resource under-utilization when the MAI is weak. Therefore, the overall performance would degrade significantly. On the flip side, the MAI self-similarity, by definition, implies the existence of a nontrivial MAI temporal correlation structure. This correlation structure can be exploited for efficient resource allocation at coarse time scales, such as rate control and admission control.

Proof: The proof uses results of [46], so we adopt their notation when possible. Recall that the intracell MAI is given by $\sum_{k\in C_1,k\neq 1}\bar{P}g'_{k,1}(t)X_{k,1}(t)$ and the intercell MAI from cell i is $\sum_{k\in C_i}P_{k,i}(t)g_{k,1}(t)X_{k,i}(t)$. Our proof focuses on the intercell MAI, and it is clear that the characterization of the intracell MAI follows the same line (and is less involved). Note that $H=(3-\alpha_{\min})/2$.

Consider the intercell MAI from cell i ($i\neq 1$), and rewrite it as $\mathcal{I}_{1,i}(t)=\sum_{k=1}^{K_i}P_{k,i}(t)g_{k,1}(t)X_{k,i}(t)$. The interference processes $\{P_{ki}g_{k,1}X_{ki}, k=1,\ldots,K_i\}$ are i.i.d. stationary processes with finite covariance functions. We want to establish a central limit theorem as $W\to\infty$. Since $K_i=\beta_i W$, we need to subtract the mean and divide by $W^{1/2}$. It is clear that the limit of the centered scaled sum will be a Gaussian process, say denoted by $G(t)$ (see, e.g., [49, 35]).

Now consider the typical summand $P_{k,i}(t)g_{k,1}(t)X_{k,i}(t)$ in (2), corresponding to the individual interference process for $k\in C_i$ and$i=1,\ldots,J$, except the desired user. First, we compute its variance and show that

$$V_{k,i}(t)\triangleq \text{Var}\left(\int_0^t P_{k,i}(u)g_{k,1}(u)X_{ki}(u)\ du\right)\sim c_0\ t^{2H},\quad \text{as } t\to\infty, \tag{8}$$

where c_0 is some positive constant. In the computations below, we drop the indices and write simply, $P(t) = P_{k,i}(t), g(t) = g_{k,1}(t), X(t) = X_{k,i}(t), \varrho(t) = \varrho_{k,1}(t)$.

Let $\gamma(t)$ denote the correlation function of $X(t)$ and $\zeta(t)$ denote the correlation function of $P(t)X(t)$. (We note that $\gamma(t)$ is the correlation function of the ON/OFF traffic flow and $\zeta(t)$ is used only for the purpose of the proof.) To this end, we have:

$$
\begin{aligned}
& V_{k,i}(t) \\
= \;& \mathrm{Var}\left(\int_0^t g(u)P(u)X(u)\ du\right) \\
= \;& \mathbb{E}\left[\int_0^t\int_0^t X(u)P(u)g(u)X(s)P(s)g(s)\ du\ ds\right] - \left(\mathbb{E}\left[\int_0^t X(u)P(u)g(u)\ du\right]\right)^2 \\
\overset{(a)}{=} \;& \int_0^t\int_0^t \mathbb{E}[X(u)P(u)X(s)P(s)]\mathbb{E}[g(u)g(s)]\ du\ ds - t^2\left(\mathbb{E}[P(0)X(0)]\right)^2\left(\mathbb{E}[g(0)]\right)^2 \\
= \;& \int_0^t\int_0^t \left\{\mathbb{E}[P(u)X(u)P(s)X(s)] - \left(\mathbb{E}[X(0)P(0)]\right)^2\right\}\left\{\mathbb{E}[g(u)g(s)] - \left(\mathbb{E}[g(0)]\right)^2\right\} duds \\
& + \left(\mathbb{E}[g(0)]\right)^2\int_0^t\int_0^t \left\{\mathbb{E}[P(u)X(u)P(s)X(s)] - \left(\mathbb{E}[P(0)X(0)]\right)^2\right\}\ du\ ds \\
& + \left(\mathbb{E}[P(0)X(0)]\right)^2\int_0^t\int_0^t \left\{\mathbb{E}[g(u)g(s)] - \left(\mathbb{E}[g(0)]\right)^2\right\}\ du\ ds \\
\overset{(b)}{=} \;& \mathrm{var}(P(0)X(0))\ \mathrm{var}(g(0))\ \int_0^t\int_0^t \zeta(u-s)\varrho(u-s)\ du\ ds \\
& + \left(\mathbb{E}[g(0)]\right)^2\ \mathrm{var}(P(0)X(0))\ \int_0^t\int_0^t \zeta(u-s)\ duds \\
& + \left(\mathbb{E}[P(0)X(0)]\right)^2\ \mathrm{var}(g(0))\ \int_0^t\int_0^t \varrho(u-s)\ du\ ds \\
\overset{(c)}{=} \;& 2\ \mathrm{var}(P(0)X(0))\ \mathrm{var}(g(0))\int_0^t\int_0^v \zeta(u)\varrho(u)\ du\ dv \\
& + 2\left(\mathbb{E}[g(0)]\right)^2\ \mathrm{var}(P(0)X(0))\int_0^t\int_0^v \zeta(u)\ du\ dv \\
& + 2\left(\mathbb{E}[P(0)X(0)]\right)^2\mathrm{var}(g(0))\int_0^t\int_0^v \varrho(u)\ du\ dv, \qquad (9)
\end{aligned}
$$

where (a) follows from Condition 2 and the independence between the fading process and the ON/OFF traffic flow, (b) from the stationarity of the $P_{k,i}(u)$, $g_{k,1}(u)$ and $X_{k,i}(u)$, and (c) from the even symmetry property of correlation functions.

Next, we characterize the correlation function of $P(u)X(u)$, denoted $\zeta(u)$. Following [46], define $\pi(u) = \Pr$ (the user is ON at time u | the user is ON at time 0). Let μ_p denote the mean of $P(u)$. Observe that

$$
\begin{aligned}
& \zeta(u)\cdot\mathrm{var}(P(0)\mathrm{var}(X(0)) \\
= \;& \mathbb{E}[P(u)X(u)P(0)X(0)] - \left(\mathbb{E}[X(0)P(0)]\right)^2 \\
= \;& \mathbb{E}[P(u)P(0)]\ \ \Pr(\text{ times u and 0 are in the same ON-period}) - \left(\mu_p\frac{\mu_1}{\mu_1+\mu_2}\right)^2
\end{aligned}
$$

$$
\begin{aligned}
&= \mathbb{E}[P(u)P(0)]\pi(u)\frac{\mu_1}{\mu_1+\mu_2} - \left(\mu_p\frac{\mu_1}{\mu_1+\mu_2}\right)^2 \\
&= \frac{\mu_1}{\mu_1+\mu_2}\left\{\left[\mathbb{E}[P(u)P(0)] - \mu_p^2\right]\left(\pi(u) - \frac{\mu_1}{\mu_1+\mu_2}\right)\right\} \\
&\quad + \left(\frac{\mu_1}{\mu_1+\mu_2}\right)^2\left[\mathbb{E}[P(u)P(0)] - \mu_p^2\right] + \frac{\mu_1}{\mu_1+\mu_2}\mu_p^2\left(\pi(u) - \frac{\mu_1}{\mu_1+\mu_2}\right) \\
&= \frac{\mu_1}{\mu_1+\mu_2}\left[\mathrm{var}(P[0])\mathrm{var}(X(0))\vartheta(u)\gamma(u) + \mu_p^2\mathrm{var}(X(0))\gamma(u) + \frac{\mu_1}{\mu_1+\mu_2}\mathrm{var}(P[0])\vartheta(u)\right] \quad (10)
\end{aligned}
$$

Appealing to [46, Theorem 1], we obtain that

$$\int_0^t\int_0^v \gamma(u)\ du\ dv \sim c_1\ t^{2H} \quad \text{as} \ \ t\to\infty, \tag{11}$$

where c_1 is some positive constant. Recall from Condition 2 that

$$\varrho(u) \sim o(u^{2H-2}) \ \text{ and } \ \vartheta(u) \sim o(u^{2H-2}) \ \text{ as } \ u\to\infty. \tag{12}$$

We have that

$$\int_0^t\int_0^v \vartheta(u)\ du\ dv = \int_0^t\int_0^v o\left(u^{2H-2}\right)\ du\ dv = o(t^{2H}); \tag{13}$$

and

$$
\begin{aligned}
\int_0^t\int_0^v \vartheta(u)\gamma(u)\ du\ dv &= \int_0^t\int_0^v o\left(u^{4H-4}\right)\ du\ dv &(14)\\
&= o(t^{4H-2}) = o(t^{2H}). &(15)
\end{aligned}
$$

It follows that

$$\int_0^t\int_0^v \zeta(u)\ du\ dv \sim c_2\ t^{2H} \quad \text{as} \ \ t\to\infty; \tag{16}$$

and

$$\int_0^t\int_0^v \varrho(u)\zeta(u)\ du\ dv = o(t^{2H}). \tag{17}$$

Then, combining (9), (10), (16), and (17) yields that

$$V_{k,i}(t) \sim c_0\ t^{2H}, \quad \text{as } t\to\infty. \tag{18}$$

Having shown that $V_{k,i}(t) \sim c_0\ t^{2H}$, next we show that after appropriate normalization, $\int_0^{Tt}\mathcal{I}_{1,i}(u)\ du$ is a fractional Brownian motion. By applying the central limit theorem, mentioned at the beginning of the proof, it is clear that the following process

$$\frac{1}{W^{1/2}}\left(\mathcal{I}_{1,i}(u) - \mathbb{E}\left[\mathcal{I}_{1,i}(u)\right]\right) = \sqrt{\frac{\beta_i}{K_i}}\sum_{k=1}^{K_i}\left[P_{k,i}(u)g_{k,1}(u)X_{k,i}(u) - \mathbb{E}\left[P(0)X(0)\right]\mathbb{E}\left[g(0)\right]\right] \tag{19}$$

converges, as a process in the variable u, in distribution to a Gaussian process $\{G(u), u\geq 0\}$. Since the process before the limit is stationary, so is the limiting Gaussian process $\{G(u), u\geq 0\}$. The integral $\int_0^{Tt}G(u)\ du$ is therefore Gaussian and has stationary increments. By the previous

calculations, the variance of $\int_0^{Tt} G(u)\ du$ is asymptotically equivalent, as $T \to \infty$, to $c_0(Tt)^{2H}$. By applying the results in [9], it follows that $T^{-H}\int_0^{Tt} G(u)\ du$ converges, as $T \to \infty$, to a fractional Brownian motion. We conclude that for large W and T, $\frac{1}{T^H W^{1/2}}\int_0^{Tt} \mathcal{I}_{1i}(u)\ du$ behaves statistically like $\sqrt{c_1}B_H(t)$, where $B_H(t)$ is a fractional Brownian motion with Hurst parameter $H = (3-\alpha_{\min})/2$ and c_1 is some constant (cf. [46]). More precisely, we have that

$$\mathcal{L}\lim_{T\to\infty}\mathcal{L}\lim_{W\to\infty}\frac{\int_0^{Tt}\mathcal{I}_{1,i}(u)\ du - TtK_i\mathbb{E}[X(0)]\mathbb{E}[h(0)]}{T^H W^{1/2}} = \sqrt{c_1}B_H(t), \tag{20}$$

where $\mathcal{L}\lim$ means convergence in the sense of the finite-dimensional distributions. This completes the proof of part a).

A simple application of [46, Theorem 2] yields part b). ∎

The $\mathcal{L}\lim_{T\to\infty}$ in Theorem 4.1 means convergence in the sense the finite-dimensional distributions. By showing the tightness along the lines of [46], we can easily establish a stronger result—weak convergence, i.e., the convergence of probability measures in the space of bounded continuous functions. We have the following corollary.

Corollary 4.1 *Suppose that Conditions 1 and 2 hold. Then, as both T and W go to infinity, the (normalized) total accumulated MAI, $T^{-H}W^{-1/2}\int_0^{Tt}\sum_{i=1}^J \mathcal{I}_{1,i}(u)\ du$, converges weakly to a fractional Brownian motion with Hurst parameter $H = (3-\alpha_{\min})/2$.*

4.2 MAI Self-Similarity in the Downlink

Recall that in the downlink, the MAI due to the users in cell i, denoted $\boldsymbol{I}_{1,i}$, is given by

$$\boldsymbol{I}_{1,i}(t) = \left(\sum_{k\in C_i} P_{k,i}(t)X_{k,i}(t)\right) g_{1,i}(t),$$

and the total MAI is $\sum_{i=1}^J \boldsymbol{I}_{1,i}(t)$. Recall that the system parameters in the downlink, including $g_{1,i}(t)$ and $P_{k,i}(t)$, are different from the corresponding ones in the uplink. Along the same lines of the proof of Theorem 4.1, we can show that $\sum_{k\in C_i} P_{k,i}(t)X_{k,i}(t)$ is self-similar. Just as in (20), when the number of users tends to infinity and at large time scales, this process converges to a fractional Brownian motion. However, the factor $g_{1,i}(t)$ in the MAI process is now common for all users in cell i. This indicates that, depending on the statistics of the fading process, there might be strong correlation between the summands of the MAI.

We expect that the MAI from the users in cell i is self-similar under mild conditions because it is the product of $\sum_{k\in C_i} P_{k,i}(t)X_{k,i}(t)$ and $g_{1,i}(t)$. However, we cannot hope that it can be approximated by a fractional Brownian motion or even a Gaussian process. Nevertheless, we show that the downlink MAI is asymptotically second-order self-similar. To this end, we impose the following regularity condition on the fading process and transmission power:

Condition 3 The sample paths of the fading process $g_{1,i}(t)$ are continuous, for $i = 1, \cdots, J$.

Condition 4 The empirical distribution of the transmission powers of the users in cell i, converges weakly to a distribution function $F_{p,i}$ with mean $\mu_{p,i}$, for $i = 1, \cdots, J$.

Theorem 4.2 (MAI Self-Similarity in Downlink) *Suppose that Conditions 1—4 hold. Then, as both W and T increase,*

a) The normalized accumulated MAI from cell i, $\{T^{-H}W^{-1/2}\int_0^{Tt} \boldsymbol{I}_{1,i}(u)du,\ t \geq 0\}$ converges in the sense of finite-dimensional distributions to a second-order self-similar process with Hurst parameter $H = (3 - \alpha_{\min})/2$.

b) The normalized total accumulated MAI, $\{T^{-H}W^{-1/2}\int_0^{Tt}\sum_{i=1}^{J} \boldsymbol{I}_{1,i}(u)\ du,\ t \geq 0\}$, converges in the sense of finite-dimensional distributions to a second-order self-similar process with Hurst parameter $H = (3 - \alpha_{\min})/2$.

Remarks: Intuitively speaking, the asymptotic self-similarity of the downlink MAI process implies that the MAI exhibits long-range dependence at coarse time scales, i.e., there are extended periods of either strong or weak interference. Comparing Theorems 4.1 and 4.2, the two results reveal that macroscopically, the downlink and uplink MAI processes appear to behave statistically differently even though they both exhibit self-similarity. It would be interesting to explore the consequences of this dichotomy in future work.

Proof: We provide a proof of part a) in the following. Part b) follows by using [46, Theorem 2].

To this end, it is sufficient to show that the asymptotic self-similarity holds for the intercell and intracell MAI for cell i, for $i = 1, \cdots, J$. We now proceed to prove (a) for the intercell MAI. The proof for the intracell MAI follows similar arguments and is omitted for brevity. For convenience, define

$$\begin{aligned}\boldsymbol{U}_{K_i}(t) &\triangleq \sum_{k\in C_i} P_{k,i}(t)X_{k,i}(t),\\ \tilde{\boldsymbol{U}}_{K_i}(t) &\triangleq \frac{1}{\sqrt{K_i}}\left(\boldsymbol{U}_{K_i}(t) - \mathbb{E}[\boldsymbol{U}_{K_i}(t)]\right),\end{aligned}$$

and for any $x > 0$,

$$\boldsymbol{S}_{K_i}(x) \triangleq \int_0^x g_{1,i}(t)\tilde{\boldsymbol{U}}_{K_i}(t)dt.$$

First consider $x \in [0, 1]$. By the central limit theorem, $\tilde{\boldsymbol{U}}_{K_i}(t)$ converges weakly, as $K_i \to \infty$, to a Gaussian process with mean zero. We note that weak convergence here is interpreted as weak convergence of probability measures on $C[0, 1]$ with the uniform topology. Let $\tilde{\boldsymbol{U}}(t)$ denote the corresponding limiting Gaussian process, and define the process

$$\boldsymbol{S}(x) \triangleq \int_0^x g_{1,i}(t)\tilde{\boldsymbol{U}}(t)dt.$$

Then the accumulated MAI from cell i over the interval $[0, x]$ is given by

$$\frac{1}{\sqrt{K_i}}\int_0^x \boldsymbol{I}_{1,i}(t)dt = \int_0^x g_{1,i}(t)\tilde{\boldsymbol{U}}_{K_i}(t)dt + \frac{1}{\sqrt{K_i}}\int_0^x g_{1,i}(t)\mathbb{E}[\boldsymbol{U}_{K_i}(t)]dt$$

$$= \boldsymbol{S}_{K_i}(x) + \frac{1}{\sqrt{K_i}} \int_0^x g_{1,i}(t)\mathbb{E}[\boldsymbol{U}_{K_i}(t)]dt$$
$$= \boldsymbol{S}_{K_i}(x) + \frac{1}{\sqrt{K_i}} \frac{\mu_1}{\mu_1+\mu_2} \int_0^x g_{1i}(t) \sum_{k=1}^{K_i} \mathbb{E}[P_{k,i}(t)]dt. \tag{21}$$

A direct application of the monotone convergence theorem [41] yields that

$$\lim_{K_i\to\infty} \frac{1}{K_i} \int_0^x g_{1i}(t) \sum_{k=1}^{K_i} \mathbb{E}[P_{k,i}(t)]dt = \mu_{p,i} \int_0^x g_{1i}(t)dt.$$

Furthermore, by Condition 2, it is straightforward to see that

$$\text{var}\left[\int_0^x g_{1i}(t)dt\right] \sim o(x^{2H}) \quad \text{as } x \to \infty. \tag{22}$$

Therefore, it suffices to characterize $\text{var}[\boldsymbol{S}_{K_i}(x)]$ as $K_i \to \infty$ and $x \to \infty$.

Next, we show, by constructing the processes on a common probability space[1], that $\boldsymbol{S}_{K_i}(x)$ converges weakly to the process $\boldsymbol{S}(x)$. Recall that we assume that x is in a finite interval $[0,1]$ (later we will elaborate on the case when x ranges over $[0,\infty)$). By Condition 3, $g(t)$ is bounded for $0 < t \le x$. Since $\tilde{\boldsymbol{U}}_{K_i}(t)$ converges weakly to $\tilde{\boldsymbol{U}}(t)$, by appealing to Skorohod's Representation [5, Theorem 25.6] (see also [43, Theorem 3; p. 357]), there exists a probability space supporting $\tilde{\boldsymbol{U}}^*_{K_i}(t)$, $K_i = 1, 2, ...$ and $\tilde{\boldsymbol{U}}^*(t)$ jointly (where $\tilde{\boldsymbol{U}}^*_{K_i}(t) \stackrel{d}{=} \tilde{\boldsymbol{U}}_{K_i}(t)$ and $\tilde{\boldsymbol{U}}^*(t) \stackrel{d}{=} \tilde{\boldsymbol{U}}(t)$), so that $\sup_{0\le t\le 1} |\tilde{\boldsymbol{U}}^*_{K_i}(t) - \tilde{\boldsymbol{U}}^*(t)| \to 0$ as $K_i \to \infty$, almost surely. (We have used $\stackrel{d}{=}$ to denote equality in distribution.) Since $g_{1,i}(t)$ is independent from the $\tilde{\boldsymbol{U}}_{K_i}(t)$'s, we can enlarge the probability space to support this $g(t)$ as well. Then, the continuity of $g_{1,i}(t)$ assures that

$$\sup_{0\le x\le 1} \left| \int_0^x g_{1,i}(t)\tilde{\boldsymbol{U}}_{K_i}(t)dt - \int_0^x g_{1,i}(t)\tilde{\boldsymbol{U}}(t)dt \right|$$
$$\stackrel{d}{=} \sup_{0\le x\le 1} \left| \int_0^x g_{1,i}(t)\tilde{\boldsymbol{U}}^*_{K_i}(t)dt - \int_0^x g_{1,i}(t)\tilde{\boldsymbol{U}}^*(t)dt \right| \to 0, \tag{23}$$

as $K_i \to \infty$, which dictates directly that $\boldsymbol{S}_{K_i}(x)$ converges to $\boldsymbol{S}(x)$, for $0 < x < 1$. Now let us turn to the case when x ranges over $[0,\infty)$. Since weak convergence on $C[0,\infty)$ is, by definition, convergence with respect to the topology of uniform convergence on each finite interval (see, e.g., [53, p. 500]), a process $\{\boldsymbol{S}_{K_i}(x), x > 0\}$ converges weakly to $\{\boldsymbol{S}(x), x > 0\}$ if and only if for each $x < \infty$, $\{\boldsymbol{S}_{K_i}(t), 0 < t \le x\}$ converges weakly to $\{\boldsymbol{S}(t), 0 < t \le x\}$. We conclude that $\{\boldsymbol{S}_{K_i}(x), x > 0\}$ converges weakly to the process $\{\boldsymbol{S}(x), x > 0\}$.

It remains to show that $\text{var}[\boldsymbol{S}(x)] \sim \ell_4 x^{2H}$ as $x \to \infty$ for some constant ℓ_4. Recall that

$$\boldsymbol{S}(x) = \int_0^x g_{1i}(t)\tilde{\boldsymbol{U}}(t)dt \tag{24}$$

Let Ξ denote the correlation function of $\boldsymbol{U}$. Using the same techniques as in the proof of Theorem 4.1, we have that

$$\text{var}[\boldsymbol{S}(x)] = 2\ \text{var}(\boldsymbol{U}(0))\ \text{var}(g_{1,i}(0)) \int_0^x \int_0^v \Xi(u)\varrho(u)\ du\ dv \tag{25}$$

[1] This is so called "the method of a single probability space" [43].

$$+ 2\left(\mathbb{E}[g_{1,i}(0)]\right)^2 \ \mathrm{var}(\boldsymbol{U}(0)) \int_0^x \int_0^v \Xi(u)\ dudv \tag{26}$$

Since

$$\int_0^x \int_0^v \Xi(u)\ dudv \sim c_3 x^{2H},$$

it follows that

$$\mathrm{var}[\boldsymbol{S}(x)] \sim \ell_4 x^{2H}, \ \text{ as } x \to \infty$$

We conclude that as both T and W go to infinity, the normalized MAI from cell i, $T^{-H}W^{-1/2}\int_0^{Tt} \boldsymbol{I}_{1,i}(u)du$ is asymptotically self-similar with the Hurst parameter $H = (3 - \alpha_{\min})/2$ (see, e.g., [40]).

∎

4.3 Extensions of Basic Models

- *Multiple antenna systems:* So far we have considered only a basic model—the MAI process in a single-antenna frequency-flat fading channels. It is straightforward to generalize the above study to multiple antenna systems in multipath fading channels. As is evident in the proofs of Theorems 4.1 and 4.2, the MAI behaves asymptotically self-similar as long as the correlation function of the fading processes is of $o(u^{2H-2})$ as $u \to \infty$. In addition, the delay spread for multipath fading is typically on the order of symbol intervals, which is much smaller than the coarser time scales (larger than the packet length) used to "measure" the MAI self-similarity. Accordingly, it is easy to see that Condition 2 on the correlation functions of the fading processes is satisfied.

- *Hybrid data/voice systems:* As a related note, we have also examined the impact of voice traffic on the MAI temporal structure in hybrid multimedia systems, though we have not presented it here. As expected, when the MAI can be effectively characterized by self-similar models, the impact of voice traffic is not significant since voice can be effectively modelled as a Markov source. Our intuition is that Markov sources exhibit only short-range dependence and would not impact long-range dependence properties.

5 Discussion on the Utility of MAI Self-Similarity in Adaptive Resource Allocation

In the preceding section, we have established that the MAI process, in both the uplink and the downlink, is asymptotically self-similar. The MAI self-similarity (with $1/2 < H < 1$), by definition, dictates that the MAI is long-range dependent. Intuitively speaking, the MAI long-range dependence indicates that there are extended periods of either strong or weak interference, and the MAI levels are highly correlated at coarser time scales. Therefore, there exists a predictive MAI temporal structure. More importantly, *the predictive MAI temporal structure can be utilized for resource allocation to achieve high spectral efficiency.* We emphasize that in particular, our findings show that the intercell

MAI is long-range dependent (even when ideal orthogonal codes are used to eliminate intra-cell MAI), and that the MAI temporal structure is especially useful for suppressing the intercell MAI. Notably, recent work [33, 48] has exploited the long-range dependence of network traffic for traffic management.

We expect that transport protocol features, particularly TCP, may have a significant impact on the short time-scale dynamics of the MAI process. This work does not account for such modifications of the MAI dynamics over fine time scales. It would be interesting to explore the practical implications of TCP-related effects on the MAI process for wireless data communications in future work.

As noted before, since our MAI model takes into account both traffic burstiness and time-varying channel conditions, the adaptive resource allocation based on the MAI prediction deals with changes of time-varying parameters, in an integrated manner. As pointed out in [20], *adaptation* is one of the underlying aspects that tie the integrated design of the network layer and physical layer in wireless networks. In particular, the MAI long-range dependence can be utilized for adaptive rate control and admission control.

- *Time scale for exploiting MAI long-range dependence:* A critical task is to identify the time scales over which MAI long-range dependence exists. Depending on the file sizes, transmission rate and fading channel parameters, such time scales can vary from tens of milliseconds to a few seconds. We expect that in future wireless systems with multiple antenna arrays, the optimal time scale for exploiting the MAI long-range dependence is on the order of tens of milliseconds because the transmission rate is relatively higher in such systems.

- *Rate control:* Rate control is a central technique for interference management in CDMA networks, and can be used as a platform for adaptive resource allocation. Since the MAI exhibits scale-invariant burstiness at multiple time scales, the "DC" component of the MAI can be either strong or weak for a relatively long period (cf. [48]). Therefore, for systems with fixed transmission rates, there exist concentrated periods where performance is poor (strong MAI) or resources are under-utilized (weak MAI). Moreover, we would expect that performance degrades further when the data burstiness increases. The intuition is as follows: the more bursty the data streams are, the "longer" the concentrated periods of poor performance or under-utilization. This necessitates rate control using the MAI prediction (see the example in the next section).

- *Admission control:* The MAI long-range dependence can also be utilized for admission control. For example, suppose a data user has a delay constraint D. Given a time window T_m for MAI prediction, if the file size is small relative to T_m, then the base station can make use of the predictive structure of MAI to 1) estimate the interference level in the next D/T_m intervals, each with length T_m, and 2) admit the new user in the time interval with a low interference level. If the file size is large, then it appears plausible to admit the new user and apply full-fledged adaptive rate control with interference prediction engaged. It is of interest to investigate the effectiveness of this intuitively appealing admission control scheme in future work.

- *Energy efficiency versus delay:* Since the battery life is a major concern for wireless devices, the MAI long-range dependence can be exploited to achieve a good balance between energy-efficiency and delay. Loosely speaking, multimedia traffic can be classified into two broad categories—*elastic* and *stream*. Elastic traffic (e.g., data files, texts or pictures) is delay tolerant, providing great flexibility for adaptive resource allocation. A simple example is that a data user can judiciously transmit only at predicted low MAI levels, using the MAI prediction techniques mentioned above. It is worth noting that the energy-efficient transmission will change the user activity and hence may change the traffic statistics.

- *Joint power control and rate control:* Roughly speaking, rate control provides a means for resource allocation at coarser time scales, whereas power control focuses more or less on symbol-level resource allocation. Motivated by the two-tier power control scheme proposed in CDMA2000 [1] (see also IS-95 standards), we can carry out transmission rate adaptation using the MAI long-range dependence at the outer loop, and implement power control in the inner loop.

6 Numerical Results

In this section, we provide numerical examples to illustrate the MAI self-similarity and its implication on transmission rate control. We consider a cellular network with each hexagonal cell having six neighboring cells. Following [55], we assume that each user's ON and OFF periods have Pareto distributions. For an ON period, the distribution of its length T is given by

$$\text{Prob}\{T > t\} = \left(\frac{T_{\min}}{t}\right)^{\alpha}, \tag{27}$$

where $T_{\min}$ corresponds to the minimum file size. We choose α to be 1.3 and $T_{\min}$ to be 0.2 s (seconds) [6, 55]. In the case of OFF periods, we choose α to be 1.5 and $T_{\min}$ to be 2 s, because $T_{\min}$ is mainly determined by the user's thinking time [7]. We also note that users' thinking time can be very different in wireless applications from in wireline applications.

For the fading channel model, we assume that fading is due to distance-related attenuation and log-normal shadowing. More specifically, our fading model is as follows: The propagation attenuation is in the form of d^{-4}, where d is the distance, and the slow-shadowing fading is log-normal with standard deviation $\sigma_\Omega = 8$dB. We use Gudmundson's AR model in (6) for log-normal shadowing, that is,

$$\Omega_{n+1} = \xi\Omega_n + (1-\xi)v_n, \tag{28}$$

with $T_f = 0.2$s and $\xi = 0.95$.

The MAI is generated for $1,000$ seconds and "measured" at a 10ms granularity. We assume that the total number of ON/OFF users in cell j, $K_j = 120$, for $j = 1, \cdots, 7$. We note that the average number of active (ON) users per cell is around 15 [1], and the average throughput per cell is around 1.5 Mb/s. Note that current 3G standards can support 2.4 Mb/s.

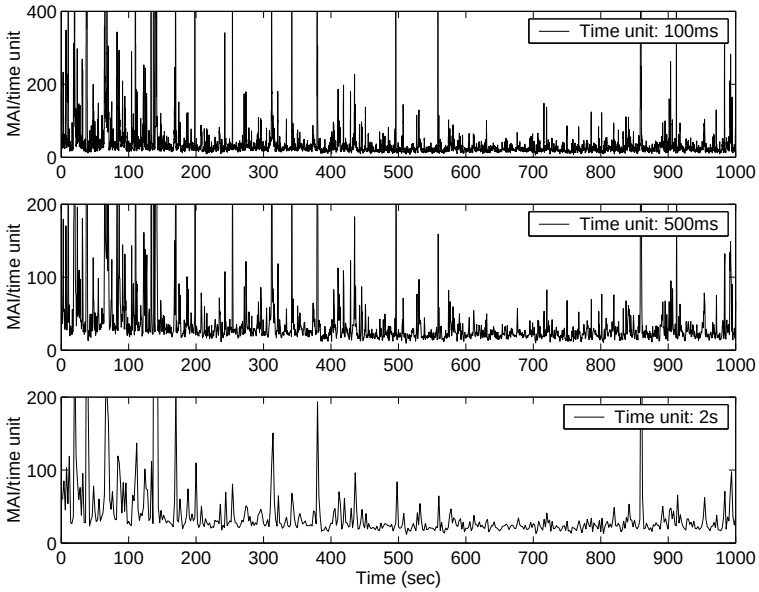

Figure 2: *Pictorial "proof" of MAI self-similarity in the uplink: normalized MAI per time unit on three time scales (100ms, 500ms, 2s).*

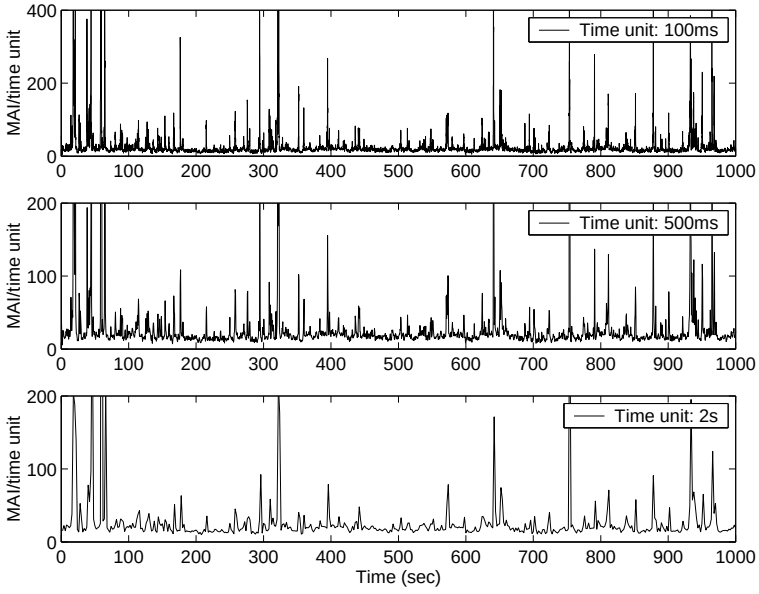

Figure 3: *Pictorial "proof" of MAI self-similarity in the downlink: normalized MAI per time unit on three time scales (100ms, 500ms, 2s).*

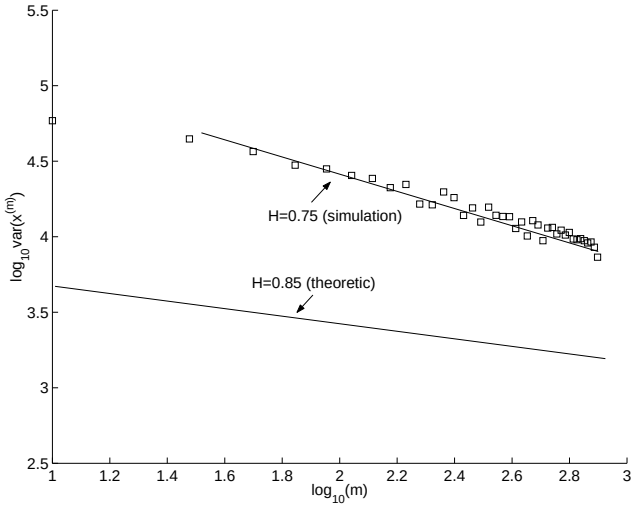

Figure 4: *Estimating self-similarity index H of the MAI process in the uplink via the variance method*

6.1 MAI Self-Similarity Phenomenon

Figures 2 and 3 depict sequences of simple plots of average MAI for three different choice of time units, in the uplink and downlink, respectively. Specifically, for the uplink, the MAI sequence $\{\mathcal{I}_n, n = 1, 2, \cdots, N\}$ is simulated and aggregated over different time scales. Parameter m corresponds to a time scale of $10 \cdot m$ ms, and the resulted aggregated sequence at time scale $(10m)$ ms is given by [45]:

$$\mathcal{I}_i^{(m)} = \frac{1}{m}(\mathcal{I}_{im-m+1} + \cdots + \mathcal{I}_{im}), \quad i = 1, 2, \cdots, [N/m]. \tag{29}$$

Similarly, for the downlink, the MAI sequence $\{\boldsymbol{I}_n, n = 1, 2, \cdots, N\}$ is simulated and aggregated over different time scales. As is evident in Figures 2 and 3, the MAI exhibits scale-invariant burstiness at multiple time scales and is self-similar. We note that in the above calculations we have used the notion of second-order self-similarity for discrete random processes.

A key parameter associated with self-similar processes is the *Hurst parameter*, with range $1/2 \leq H < 1$. Indeed, The Hurst parameter H is sometimes called self-similarity index. Estimating H plays a crucial role in diagnosing long range dependence. Figures 4 and 5 give the results by using the variance method to estimate H [45]. Specifically, in the variance method, we compute the sample variance at time scale $(10m)$ ms:

$$\text{var}(\mathcal{I}_i^{(m)}) = \frac{1}{[N/m]} \sum_{i=1}^{[N/m]} \left(\mathcal{I}_i^{(m)} - \bar{\mathcal{I}}\right)^2,$$

where $\bar{\mathcal{I}}$ is the sample mean of the whole sequence $\{\mathcal{I}_n, n = 1, 2, \cdots, N\}$. As shown in Figures 4 and 5, the estimated Hurst parameter is 0.75 in the uplink case, and is 0.76 in the downlink case, corroborating the result given by Theorems 4.1 and 4.2 that the aggregated MAI is self-similar at coarser time scales.

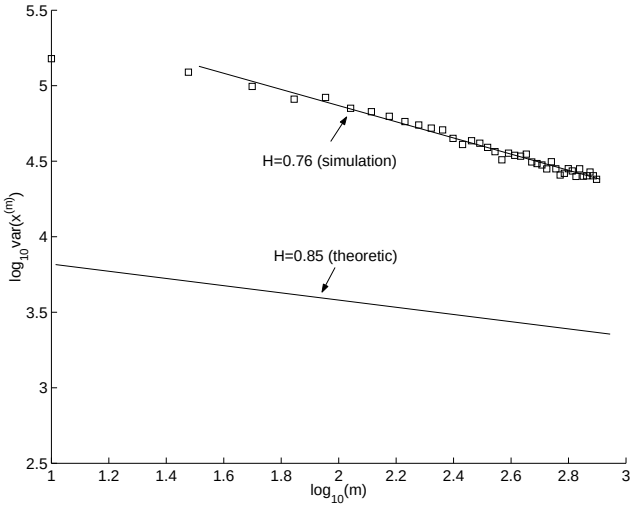

Figure 5: *Estimating self-similarity index H of the MAI process in the downlink via the variance method*

6.2 A simple Application: MAI Self-Similarity Based Rate Control

The MAI self-similarity, by definition, implies the existence of a temporal correlation structure, which can be exploited for efficient resource allocation. Thus motivated, we have devised an easy-to-implement rate adaptation scheme based on the MAI self-similarity in the downlink. The underlying rationale can be summarized as follows: If the (predicted) future interference is weak, we increase the transmission rate via decreasing the spreading gain or increasing code rate or a combination thereof. If the predicted future MAI is strong, we throttle the transmission rate downward accordingly. It is worth noting that the MAI prediction is *measurement-based* and therefore easy-to-implement.

It is clear that the MAI prediction is a key ingredient of our rate adaptation scheme. We note that in this example, the rate adaptation is implemented at the packet level. Since the MAI self-similarity indicates that there exists a predictive structure of the MAI at coarser time scales, it is natural to expect that the MAI prediction utilizing the MAI self-similarity can improve prediction accuracy. Therefore, we devise a multiple time-scale MAI predictor, which combines the packet-level and large time-scale predictions. More specifically, our prediction algorithm optimally combines interference prediction at two time scales, one at the packet level and the other at a larger time scale T_m, i.e.,

$$\hat{\boldsymbol{I}}_{n,p} = \lambda \boldsymbol{I}_{n-1,p} + (1-\lambda)\bar{\boldsymbol{I}}_{n-1,m}, \tag{30}$$

where $\hat{\boldsymbol{I}}_{n,p}$ is the predicted interference for the next packet, $\boldsymbol{I}_{n-1,p}$ and $\bar{\boldsymbol{I}}_{n-1,m}$ correspond to the interference prediction at the packet level and the time scale T_m, respectively, and $\lambda \in (0,1)$.

We now use the throughput as the performance metric to compare three schemes: Scheme 1 is based on the simple packet-level MAI prediction only, Scheme 2 employs the multiple time-scale MAI predictor with $T_m = 0.3$s, and Scheme 3 uses the multiple time-scale MAI predictor with $T_m = 3$s. We also choose the *maximal throughput* among all possible fixed transmission rates as a critical baseline. Figure 6 shows that rate adaptation in bursty data systems can improve system

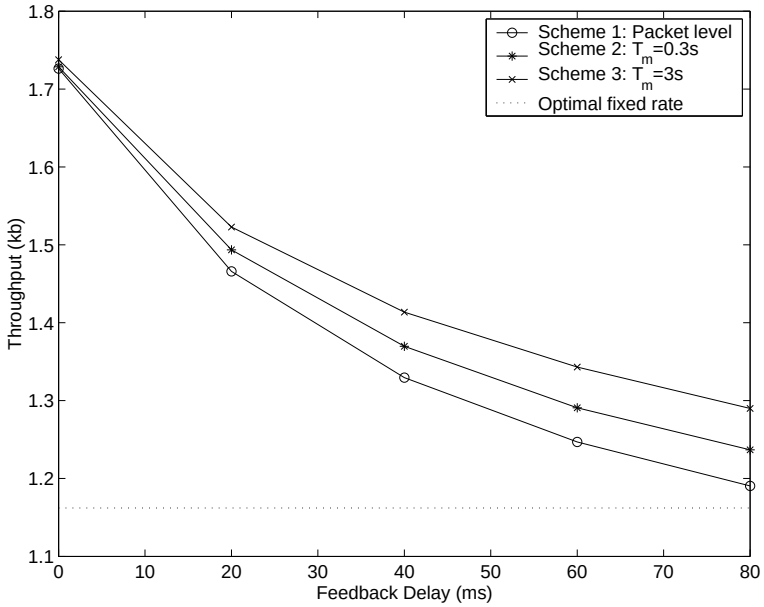

Figure 6: Throughput per 10ms versus feedback delay

performance greatly. it also shows that Scheme 3 achieves the largest throughput, then Scheme 2 and Scheme 1. The underlying rationale is that we can get more accurate MAI prediction by using the multiple time-scale prediction method. It is worth noting that the choice of the large time scale also affects the prediction accuracy.

Feedback delay may be inevitable in practical systems. Figure 6 shows that the throughput degrades as the feedback delay increases, and that Scheme 3 is significantly better than Scheme 1 when the feedback delay is large.

7 Conclusions

We have attempted to characterize the MAI in a multimedia CDMA network from a stochastic process perspective. To this end, we have first developed a MAI model that simultaneously takes into account time-varying channel conditions and the burstiness of data traffic. Our findings show that the MAI processes in both the uplink and the downlink are asymptotically self-similar. In particular, as both T (time scale) and W (bandwidth) increases, for the uplink, the MAI converges to a fractional Brownian motion, whereas for the downlink, the MAI cannot be modeled as a fractional Brownian motion. It would be interesting to explore the consequences of this dichotomy in future work.

The MAI self-similarity indicates directly the existence of a predictive MAI structure at coarser time scales. This predictive MAI structure can be exploited for adaptive resource allocation to achieve efficient interference management, which is the key to achieving high spectral efficiency. In a nutshell, we expect that the predictive MAI temporal structure exists in many multimedia CDMA systems. A few observations are worth noting: 1) The nontrivial MAI (particularly intercell MAI)

temporal correlation structure exists in many realistic systems. For instance, in a cellular CDMA network, each cell has six adjacent neighboring cells, so it is likely that there are hundreds of co-channel interferers. Therefore, the approximation of the MAI process by long-memory models holds well. 2) The MAI temporal correlation structure exists in systems with a variety of multimedia traffic, because it is the heavy-tailedness of traffic that results in the MAI temporal correlation structure. 3) Rate control would not change the MAI long-range dependence since the heavy tailed ON/OFF-durations are defined based on average rate. 4) The MAI prediction can be implemented easily based on measurements. Furthermore, for a measurement-based implementation of MAI prediction, we only need to know the existence of temporal MAI structure at coarser time scales. 5) Needless to say, the time scale for MAI prediction is an important parameter affecting predictability. Depending on the file size, transmission rate and fading channel parameters, the time scale can vary from tens of milliseconds to a few seconds.

We emphasize that the utilization of the MAI temporal correlation structure parallels and complements multiuser detection, which exploits the MAI snapshot structure at the *symbol level*, whereas resource allocation decisions, particularly rate control and admission control, are taken on *coarser time scales*. Again, we note that the MAI temporal structure has been barely explored and is not well understood. A companion paper [60] is underway to utilize the MAI self-similarity to explore resource allocation for multimedia wireless applications.

We note that our results are potentially useful to characterize the aggregated network traffic made up by many individual sources or source-destination pairs, where each individual source is allowed to generate time-varying traffic (e.g., variable bit rate sources). In this sense, our results can also be viewed as a generalization of results in [46, 55], although the system models under consideration are different.

Worth noting is that transport protocol features, particularly TCP, may have a significant impact on the short time-scale dynamics of the MAI process, and that this work does not account for such modifications of the MAI dynamics. It would be interesting to explore the practical implications of TCP-related effects on the MAI process for wireless data communications in future work.

Acknowledgements

The authors thank Professor Murad S. Taqqu for the reference [27] and Ming Hu for his kind help in obtaining some simulation results. The authors would also like to thank the anonymous reviewers for their helpful comments that greatly improved the presentation of the paper.

References

[1] "CDMA2000 (FDD MC-CDMA or G3G CDMA MC) standards," *TIA IS-2000*, 2001 (see http://tiaonline.org/standards/sfg/imt2k/cdma2000/).

[2] P. Abry, P. Flandrin, M. S. Taqqu, and D. Veitch, "Wavelets for the analysis, estimation, and synthesis of scaling data," in *Self-Similar network Traffic and Performance Evaluation* (K. Park and W. Willinger, eds.), pp. 39–88, John Wiley & Sons, Inc., 2000.

[3] J. Beran, *Statistics for Long-Memory Processes*. Chapman & Hall/CRC, 1994.

[4] E. Biglieri, G. Caire, and G. Taricco, "Limiting performance for block-fading channels with multiple antennas," *IEEE Transactions on Information Theory*, to appear, 2001.

[5] P. Billingsley, *Convergence of Probability Measures*. John Wiley & Sons, Inc., 1968.

[6] J. C.-I. Chuang and N. R. Sollenberger, "Spectrum resource allocation for wireless packet access with application to advanced cellular internet service," *IEEE Journal on Selected Areas in Communications*, vol. 16, pp. 820–829, 1998.

[7] M. E. Crovella and A. Bestavros, "Self-similarity in world wide web traffic: Evidence and possible causes," *IEEE/ACM Transactions on Networking*, vol. 5, pp. 835–846, 1997.

[8] M. E. Crovella, M. Taqqu, and A. Bestavros, "Heavy-tailed probability distributions in the world wide web," in *A Practical Guide to Heavy Tails: Statistical Techniques and Applications* (R. J. Adler, R. E. Feldman, and M. S. Taqqu, eds.), pp. 3–26, Boston: Birkhauser, 1998.

[9] Y. A. Davydov, "The invariance principle for stationary processes," *Th. Prob. Appl.*, pp. 487–498, 1970.

[10] A. Feldmann, "Chracteristics of TCP connection arrivals," in *Self-Similar network Traffic and Performance Evaluation* (K. Park and W. Willinger, eds.), pp. 367–400, John Wiley & Sons, Inc., 2000.

[11] E. Geraniotis and M. Pursley, "Performance of coherent direct-sequence spread spectrum communications over specular multipath fading channels," *IEEE Transactions on Communications*, vol. 33, pp. 502–508, June 1985.

[12] K. S. Gilhousen, I. M. Jacobs, R. Padovani, A. J. Viterbi, L. A. Weaver Jr., and C. E. Wheatley III, "On the capacity of a cellular CDMA system," *IEEE Transactions on Vehicular Technology*, vol. 40, pp. 303–312, May 1991.

[13] M. Gudmundson, "Correlation model for shadow fading in mobile radio systems," *Electronics Letters*, vol. 27, pp. 2145–2146, 1991.

[14] D. Guo, S. Verdú, and L. K. Rasmussen, "Asymptotic normality of linear multiuser receiver outputs," *preprint*.

[15] S. V. Hanly and D. Tse, "Power control and capacity of spread-spectrum wireless networks," *Automatica*, vol. 35, pp. 1987–2012, Dec. 1999.

[16] J. M. Holtzman, "A simple accurate method to calculate spread spectrum multiple access error probabilities," *IEEE Transactions on Communications*, vol. 40, pp. 461–464, Mar. 1992.

[17] M. L. Honig and V. Poor, "Adaptive interference suppression," in *Wireless Communications: Signal Processing Perspectives* (H. V. Poor and G. W. Wornell, eds.), pp. 64–128, Upper Saddle River, NJ: Prentice-Hall, 1998.

[18] B. Hughes, "Alpha-stable models of multiuser interference," in *Proceedings of International Symposium on Information Theory*, (Sorrento, Italy), p. 383, June 2000.

[19] L. Jalloul and J. M. Holtzman, "Performance analysis of DS/CDMA with noncoherent m-ary orthogonal modulation in multipath fading channels," *IEEE Journal on Selected Areas in Communications*, vol. 12, pp. 862–870, June 1994.

[20] R. H. Katz, "Adaptation and mobility in wireless information systems," *IEEE Personal Communications Magazine*, vol. 1, pp. 6–17, 1994.

[21] T. Konstantopoulos and S.-J. Lin, "Fractional brownian motions and levy processes as limits of stochastic traffic models," in *Presented at the 34th Allerton Conference*, Oct. 2–4, 1996.

[22] T. Konstantopoulos and S.-J. Lin, "Macroscopic models for long-range dependent network traffic," *Queueing Systems: Theory and Applications*, pp. 215–243, 1998.

[23] T. M. Kurtz, "Limit theorems for workload input models," in *Stochastic Networks: Theory and Applications* (F. P. Kelly, S. Zachary, and I. Ziedins, eds.), pp. 119–140, Oxford Science Publications, 1996.

[24] D. Laforgia, A. Luvison, and V. Zingarelli, "Bit error rate evaluation for spread spectrum multiple access systems," *IEEE Transactions on Communications*, vol. 32, pp. 660–669, June 1984.

[25] J. Lehnert and M. Pursley, "Error probability for binary direct-sequence spread spectrum communications with random signature sequences," *IEEE Transactions on Communications*, vol. 35, pp. 87–98, 1987.

[26] W. E. Leland, M. S. Taqqu, W. Willinger, and D. V. Wilson, "On the self-similar nature of ethernet traffic (extended version)," *IEEE/ACM Transactions on Networking*, vol. 2, pp. 1–14, 1994.

[27] J. B. Levy and M. S. Taqqu, "Renewal reward processes with heavy-tailed inter-renewal times and heavy-tailed rewards," *Bernoulli*, vol. 6, no. 1, pp. 23–44, 2000.

[28] U. Madhow and M. L. Honig, "On the average near-far resistance for MMSE detection of directed-sequence CDMA signals with random spreading," *IEEE Transactions on Information Theory*, pp. 2039–2045, Sept. 1999.

[29] T. L. Marzetta and B. M. Hochwald, "Capacity of a mobile multiple-antenna communication link in rayleigh flat fading," *IEEE Transactions on Information Theory*, vol. 45, pp. 139–157, Jan. 1999.

[30] T. Mikosch, S. Resnick, H. Rootzen, and A. Stegeman, "Is network traffic approximated by a stable Levy motion or a fractional Brownian motion?," *Annals of Applied Probability*, 1999.

[31] D. Mitra and J. A. Morrison, "A distributed power control algorithm for bursty transmissions on cellular, spread spectrum wireless networks," in *Proc. 5th WINLAB Workshop on Third Generation Wireless Information Networks* (J. M. Holtzman, ed.), pp. 201–212, Kluwer Academic Publishers, 1996.

[32] R. Morrow and J. Lehnert, "Bit-to-bit error dependence in slotted DS/SSMA packet systems with random signature sequences," *IEEE Transactions on Communications*, vol. 37, pp. 1052–1061, 1989.

[33] S. A. M. Ostring, H. R. Sirisena, and I. Hudson, "Rate control of elastic connections competing with long-range dependent network traffic," *IEEE Transactions on Communications*, vol. 48, pp. 1092–1111, 2001.

[34] V. Paxson and S. Floyd, "Wide area traffic: The failure of Poisson modeling," *IEEE/ACM Transactions on Networking*, vol. 3, pp. 226–244, 1995.

[35] V. Piterbarg, *Asymptotic Methods in the Theory of Gaussian Processes and Fields*. American Mathematics Society, 1996.

[36] H. V. Poor and S. Verdú, "Probability of error in MMSE multiuser detection," *IEEE Transactions on Information Theory*, vol. 43, no. 3, pp. 858–871, May 1997.

[37] M. Pursley, "Performance evaluation for phas-coded spread spectrum multiple access communication – part I: System analysis," *IEEE Transactions on Communications*, vol. 25, pp. 795–799, 1977.

[38] M. Pursley, D. Sarwate, and W. Stark, "Error probability for direct-sequence spread spectrum multiple access communications – part I: Upper and lower bounds," *IEEE Transactions on Communications*, vol. 30, pp. 975–984, May 1982.

[39] T. S. Rappaport, *Wireless Communications: Principles and Practice*. New Jersey: Prentice Hall, 1996.

[40] R. H. Riedi and W. Willinger, "Toward an improved understanding of network traffic dynamics," in *Self-Similar network Traffic and Performance Evaluation* (K. Park and W. Willinger, eds.), pp. 507–530, John Wiley & Sons, Inc., 2000.

[41] H. L. Royden, *Real Analysis*. Prentice Hall, Inc., third ed., 1988.

[42] G. Samorodnisky and M. S. Taqqu, *Stable Non-Gaussian Random Processes*. New York: Chamman & Hall/CRC, 1994.

[43] A. Shiryayev, *Probability*. Springer-Verlag, 1984.

[44] G. Stuber, *Principles of Mobile Communication*. Boston, MA: Kluwer, 1996.

[45] M. S. Taqqu and V. Teverovsky, "On estimating the intensity of long-range dependence in finite and infinite variance time series," in *A practical Guide to heavy Tails: Statistical Techniques and Applications* (R. J. Adler, R. E. Feldman, and M. S. Taqqu, eds.), pp. 177–218, 1998.

[46] M. S. Taqqu, W. Willinger, and R. Sherman, "Proof of a fundamental result in self-similar traffic modeling," *Computer Communications Reviews*, vol. 27, no. 2, pp. 5–23, 1997.

[47] B. Tsybakov and N. D. Georganas, "Self-similar processes in communications networks," *IEEE Transactions on Information Theory*, vol. 44, pp. 1713–1725, Sept. 1998.

[48] T. Tuan and K. Park, "Multiple time scale redundancy control for QoS-sensitive transport of real-time traffic," in *Proc. IEEE INFOCOM'2000*, (Tel-Aviv, Israel), 2000.

[49] N. N. Vakhania, *Probability Distributions on Linear Spaces*. North-Holland, New York, 1981.

[50] M. Varanasi and B. Aazhang, "Optimally near-far resistant multiuser detection in differentially coherent synchronous channels," *IEEE Transactions on Information Theory*, vol. 37, pp. 1006–1018, July 1991.

[51] S. Verdú, *Multiuser Detection*. Cambridge University Press, 1998.

[52] A. J. Viterbi, *CDMA—Principles of Spread Spectrum Communications*. Addison–Wesley, 1995.

[53] W. Whitt, *Stochastic-Process Limits*. New York: Springer-Verlag, 2002.

[54] W. Willinger, V. Paxson, and M. S. Taqqu, "Self-similarity and heavy tails: structural modeling of network traffic," in *A practical Guide to heavy Tails: Statistical Techniques and Applications* (R. J. Adler, R. E. Feldman, and M. S. Taqqu, eds.), pp. 27–54, Boston: Birkhauser, 1998.

[55] W. Willinger, M. S. Taqqu, R. Sherman, and D. V. Wilson, "Self-similarity through high-variability: Statistical analysis of ethernet LAN traffic at the source level," *IEEE/ACM Transactions on Networking*, vol. 5, pp. 71–86, 1997.

[56] X. Yang and A. P. Petropulu, "Co-channel interference modeling and analysis in a poisson field of interferers in wireless communications," *IEEE Transactions on Signal Processing*, vol. 54, pp. 64–76, Jan. 2003.

[57] K. Yao, "Error probability of asynchronous spread spectrum multiple access communication systems," *IEEE Transactions on Communications*, vol. 25, pp. 803–809, 1977.

[58] J. Zhang and E. K. P. Chong, "Linear MMSE multiuser receivers: MAI conditional weak convergence and network capacity," *IEEE Transactions on Information Theory*, pp. 2114–2122, July 2002.

[59] J. Zhang, E. K. P. Chong, and D. N. C. Tse, "Output MAI distributions of linear MMSE multiuser receivers in DS-CDMA systems," *IEEE Transactions on Information Theory*, pp. 1128–1144, Mar. 2001.

[60] J. Zhang, M. Hu, and N. B. Shroff, "Bursty data over CDMA: MAI self similarity, rate control and admission control," in *Proceedings of IEEE INFOCOM'02*, (New York, NY), pp. 391–399, 2002.

Biographies

Junshan Zhang (S'98, M'00) received his Ph.D. degree from the School of Electrical and Computer Engineering at Purdue University in 2000. He joined the Department of Electrical Engineering at Arizona State University in August 2000, where he is currently an Assistant Professor.

His research interests fall in the general area of wireless networks, spanning from the networking layer to the physical layer. His current research focuses on fundamental problems in cellular networks, wireless ad-hoc/sensor networks, including cross-layer design, scheduling, resource management, network information theory.

Dr. Zhang received a NSF CAREER award in 2003 and the Outstanding Research Award from the IEEE Phoenix Section in 2003. He was chair of the IEEE Communications and Signal Processing Phoenix Chapter from Jan. 2001 to Dec. 2003. He has served as a member of the technical program committees of INFOCOM, GLOBECOM, ICC, MOBIHOC and ITCOM. He has served as an Associate Editor for IEEE Transactions on Wireless Communications since 2004.

Takis Konstantopoulos(M'90) received the Diploma in Electrical Engineering from the National Technical University of Athens, Greece, and his Master and Ph.D. degrees from the University of California at Berkeley in 1983, 1985 and 1989, respectively.

He held the position of charge de recherche in INRIA, France, between 1989 and 1990. He has held several short and long term research and visiting positions, including at UC Berkeley, University of Maryland, Cornell University, University of Patras, Greece, the Technical University of Braunschweig, Germany, the Heriot-Watt University, Edinburgh, UK, and the Pennsylvannia State University. He is currently an associate professor with the Department of Electrical and Computer Engineering at the University of Texas at Austin. His main research interests are in performance analysis, modeling and control of communication networks, applied probability and stochastic processes, stochastic systems and operations research.

Dr. Konstantopoulos is a recipient of several NSF awards. He is currently an Associate Editor of "Queueing Systems: Theory and Applications". He is a member of IEEE, the American Mathematical Society, the Institute of Mathematical Statistics.